Supporting Information

Bonnelle et al. 10.1073/pnas.1113455109

SI Results

Neuropsychological Assessment. Compared with an age-matched control group, TBI patients showed an expected pattern of neuropsychological impairment (Table S1). A subset of 52 patients (mean age 38 ± 12) and 21 age-matched controls (mean age 39 ± 9) underwent neuropsychological assessment. As a group, TBI patients demonstrated impairments during the Verbal Fluency Letter Fluency and the Color-Word (Stroop) test, which taps inhibitory control and cognitive flexibility. Patients were slower than controls on the Color-Word test on trials requiring the ability to inhibit a prepotent response and/or to flexibly switch between alternating tasks (Table S1). They were also slower on the Trail Making Test A, which reflects impaired information processing speed. These were specific impairments limited to a subset of the behavioral measures, rather than a global impairment that spanned many domains of cognition. The patients were well matched with controls on most cognitive variables. Indeed, the patients showed better performance on a test of verbal abstract reasoning.

Behavioral Results: SSRT Is Related to Attentional Measures in Patients. As previously observed (1), SSRT was negatively correlated with accuracy on go trials in both controls ($r = -0.481$, $P = 0.023$) and patients ($r = -0.455$, $P = 0.002$). Furthermore, patients' SSRT also correlated with intraindividual variability in go RT (IIV) ($r = 0.458$, $P = 0.002$) and mean RT ($r = 0.395$, $P = 0.007$). This provides evidence that performance on stop trials is related to attentional processes that influence both go and stop trial performance.

DMN Deactivation Is Unrelated to SSRT in Controls. All control subjects showed deactivation of the precu/PCC during correct stop relative to go trials. Therefore, we were unable to divide the control subjects in the same way as we did for the patient analysis using positive or negative values for activation change on stop trials. However, groups with high and low DMN deactivation (defined with a median split of precu/PCC activity for StC > Go) showed no difference in SSRT.

SN Integrity Predicts DMN Function Independently of Lesions and Whole-Brain White Matter Damage. The binary logistic regression relating rAI–preSMA/dACC tract integrity to precu/PCC deactivation remained significant after removing the 21 subjects with focal cortical lesions ($\chi^2 = 4.7$, df = 1, $P = 0.029$). In addition, the predictive model remained significant when mean FA for the whole white matter skeleton was regressed-out from each tract's FA measures ($\chi^2 = 8.1$, df = 1, $P = 0.004$).

Additional Analysis of White Matter Tracts Connecting the rAI to EN Nodes. We found no evidence that the structure of rAI–preSMA/dACC tract correlated with activity within task-positive regions involved in executive control. To investigate whether the AI might exert control over the EN through more direct structural connections, we investigated connections to two additional right hemisphere regions, the FEF and IPS, both of which are regions often activated during executive control. Mean tracts were generated in a similar way to our other tracts, using the same ROIs used for the rFEF–rIPS tract (Table S4). Mean FA from these two tracts showed only a borderline difference to controls (rAI–rFEF, $P = 0.108$; rAI–rIPS, $P = 0.081$, corrected for multiple comparison). We found no relationship between tract structure and brain activity. When the mean FA of the tracts were used as regressors in two additional whole-brain analyses of brain activity, no brain region showed activity that was significantly correlated with tract structure.

SN Integrity Is Correlated with Stroop Performance. Further evidence that the rAI–preSMA/dACC white matter tract is important for cognitive flexibility is provided by the analysis of the pattern of neuropsychological performance across the patient group. Among the neuropsychological tests performed by patients, one is particularly useful to assess cognitive flexibility and inhibitory control: the Delis-Kaplan Executive Function System (D-KEFS) Color-Word Interference or Stroop test (2). FA within the rAI–preSMA/dACC tract (corrected for age and whole-brain white matter damage) was significantly correlated with the inhibition/switching vs. combined color naming and word reading contrast score (Spearman one tailed $r = -0.265$ $P = 0.029$ $n = 52$). The correlation remained when removing subjects with lesions ($r = -0.359$, $P = 0.020$, $n = 33$). A high score in this behavioral measure is thought to reflect both verbal inhibition and cognitive flexibility impairments (2). The integrity of this tract was not correlated with any other neuropsychological measure.

SI Subjects and Methods

TBI Patients Excluded from Analysis. Sixty-five patients with a history of TBI were recruited. Eight were not included in the imaging analyses because: (*i*) two were unable to perform the task accurately; (*ii*) five were excluded because of distortion on fMRI or DTI data that was likely due to movement artifact; and (*iii*) one patient had an unexpected neurological abnormality on the scan. Therefore, 57 patients were included in the analyses reported here (11 females, mean age 36.7 ± 11.5, range 18–62 y).

TBI Patients' Clinical Details. Injury was secondary to assaults (24%), road traffic accidents (35%), falls (21%), and sports-related injury (12%), and 8% were of unknown origin. Based on the Mayo classification system for TBI severity (3), there were 42 moderate/severe and 15 mild (probable) cases of TBI. This system integrates the duration of loss of consciousness, length of posttraumatic amnesia, lowest recorded Glasgow Coma Scale in the first 24 h, and initial neuroimaging results. Exclusion criteria were as follows: neurosurgery, except for invasive intracranial pressure monitoring (one patient); history of psychiatric or neurological illness before their head injury; history of significant previous TBI; antiepileptic medication; current or previous drug or alcohol abuse; or contraindication to MRI.

Clinical Imaging. Patients were assessed by using standard T1 MRI to assess evidence of focal brain injury and gradient echo imaging to identify microbleeds, a marker of diffuse axonal injury (4). A senior consultant neuroradiologist reviewed all study MRI scans. At the time of the study, they showed the following: 11 had residual evidence of contusions, 12 had microbleeds as demonstrated on gradient echo imaging, and 10 had evidence of both. For patients with lesions visible on T1 MR imaging, lesion maps were created by manually drawing round the lesion location using FSL. The lesions were then registered to a standard MNI 152 T1 1mm template using FLIRT, and lesion overlap images were created by using fslmaths (Fig. S5). Overlap maps show that the lesions were mainly situated in the inferior parts of the frontal lobes, including the orbitofrontal cortex, and the tem-

poral poles, following a typical lesion distribution pattern for TBI patients (5).

Neuropsychological Assessment. A detailed neuropsychological battery was used to assess cognitive function. Current verbal and nonverbal reasoning ability was assessed by using Wechsler Abbreviated Scale of Intelligence Similarities and Matrix Reasoning subtests (6). Verbal Fluency Letter Fluency and Color-Word Interference (Stroop) tests were administered from the Delis-Kaplan Executive Function System to assess cognitive flexibility, inhibition, and set-shifting (7). The Trail Making Test (forms A and B) was used to further assess executive functions (8). Working memory was assessed via the Digit Span subtest of the Wechsler Memory Scale-Third Edition (WMS-III) (9). The Logical Memory I and II subtests of the WMS-III were included as measures of immediate and delayed verbal recall. The People Test from the Doors and People Test battery was used as a measure of associative learning and recall (immediate and delayed) (10).

SST (Fig. S1). The stop signal paradigm is based on the "horse-race" model of response inhibition (11). This model proposes that response inhibition is a race between an excitatory and an inhibitory process. The speed of the excitatory process corresponds to the reaction time following the go-signal. If the excitatory process is faster than the inhibitory, the response is executed. If the inhibitory process (i.e., the process responding to the stop signal) surpasses the excitatory, the response is interrupted and successfully inhibited. Consequently, the inhibition of a response depends on the relative finishing times of the two processes subsequent to the stop signal and the primary go signal.

Staircase Adaptation Procedure. In the first run of the SST, the stop signal delay (SSD: delay between the presentation of the go signal and the stop signal) started at the mean go RT of the CRT minus 200 ms. Subsequently, the SSD was adaptively varied every two stop trials. If cumulative accuracy was >50%, the SSD was increased by 50 ms; if <50%, the SSD was decreased by 50 ms. A lower limit for SSD was set to 50 ms. With this staircase procedure, a "critical" SSD could be computed for each subject per run by averaging all trials where the probability to respond is equal to the probability to inhibit. This critical SSD represents the time delay required for the subject to succeed in withholding a response in the stop trials for half of the time. SSRT was then calculated by subtracting the critical SSD from the median go RT for each run.

Strategic Slowing Down. A frequent strategy consists of slowing down on go trials to increase the chances of successfully inhibiting the response in the case a stop signal would appear. However, it is important for the correct estimation of the SSRT that the go RT reflects the subjects' "real" RT (see below). We thus limited the ability of individuals to slow down on go trials by providing negative feedback when subjects slowed their response times and passed a threshold for the speed of their go response. Negative feedback in the form of the words "Speed up!" was presented on the screen in place of the subsequent trial each time a response was made with a reaction time above the 95th percentile of the subject's current reaction time distribution.

Estimation of the SSRT. The speed of the inhibitory process (i.e., SSRT) is most often used as a behavioral measure of stop signal response inhibition (11). The SSRT is thought to represent the latency between the occurrence of the stop signal and the beginning of the stop process. Due to the fact that successful response inhibition does not result in an observable response, it must be estimated (11). With the tracking procedure mentioned above, the SSRT can be derived by subtracting the mean SSD from the mean go RT. A slow SSRT decreases the probability that the response is successfully inhibited, which is often found in conditions such as ADHD (12).

Exclusion Criteria for SSRT Estimation. For the SSRT to be accurately estimated, the stop accuracy must be close to 50% (this is to ensure that the staircase procedure has been successful), and the strategic slowing must be within a reasonable limit. Too much slowing usually artificially lowers the SSRT estimation (13). We thus excluded subjects whose stop accuracy was not comprised within 40–60% and subjects who had a number of negative feedback higher than two SDs above the group mean. With these exclusion criteria, SSRT could not be estimated on both SST runs in 3 controls and 11 patients. The analyses involving this measure are thus reported for a sample of 22 controls and 46 patients.

MRI Acquisition. MRI data were obtained by using a Philips Intera 3.0 Tesla MRI scanner using Nova Dual gradients, a phased array head coil, and sensitivity encoding (SENSE) with an under sampling factor of 2. High-resolution images (T1-weighted MPRAGE) were acquired with the following acquisition parameters: matrix size 208 × 208; slice thickness = 1.2 mm, 0.94 mm × 0.94 mm in plane resolution, 150 slices; TR = 9.6 ms; TE = 4.5 ms; flip angle 8°. fMRI images were obtained by using a T2*-weighted gradient-echo echoplanar imaging (EPI) sequence with whole-brain coverage (TR/TE = 2,000/30; 31 ascending slices with thickness 3.25 mm, gap 0.75 mm, voxel size 2.5 × 2.5 × 5 mm, flip angle 90°, field of view (FOV) 280 × 220 × 123 mm, matrix 112 × 87). Quadratic shim gradients were used to correct for magnetic field inhomogeneities within the brain.

Paradigms were programmed by using Matlab Psychophysics toolbox (Psychtoolbox-3; www.psychtoolbox.org) and stimuli presented through an IFIS-SA system (In Vivo Corporation). Responses were recorded through a fiber-optic response box (Nordicneurolab), interfaced with the stimulus presentation PC running Matlab. Participants had two sessions of imaging: one session consisted of structural brain imaging including DTI and another of task fMRI.

Diffusion-weighted volumes with gradients applied in 64 noncollinear directions were collected. The following parameters were used: 73 contiguous slices, slice thickness = 2 mm, FOV 224 mm, matrix 128 × 128 (voxel size = 1.75 × 1.75 × 2 mm^3), b value = 1000, and four images with no diffusion weighting (b = 0 s/mm^2). Diffusion-weighted images were registered to the b = 0 image by affine transformations to minimize distortion due to motion and eddy currents and then brain-extracted by using BET (14), part of the FSL image processing toolbox (15). Voxelwise FA maps were generated by using FDT in FSL.

fMRI Analysis. Imaging analysis was performed by using FEAT (FMRI Expert Analysis Tool; Version 5.98), a part of FSL (FMRIB's Software Library; www.fmrib.ox.ac.uk/fsl) (15). Image preprocessing involved realignment of EPI images, spatial smoothing using an 8-mm full-width half-maximum Gaussian kernel, prewhitening using FILM, and temporal high-pass filtering using a cutoff frequency of 1/50 Hz. FMRIB's Linear Image Registration Tool (FLIRT) was used to register EPI functional datasets into standard MNI space by using the participant's high-resolution T1. fMRI data were analyzed by using voxel-wise time series analysis within the framework of the General Linear Model (16). To this end, a design matrix was generated with a synthetic hemodynamic response function and its first temporal derivative. Several types of events were distinguished: go correct (Go), stop correct (StC), stop incorrect, and Rest. To account for variation in the SSD across runs, we modeled events by using the timing of the SSD as the regressor for each trial. The following individual and run-specific contrast

images were generated: StC vs. Go and Go vs. Rest. The two SST runs were first analyzed separately and then combined by using fixed effects analysis. Mixed effects analysis of session and group effects was carried out using FLAME (FMRIB's Local Analysis of Mixed Effects). Final statistical images were thresholded by using Gaussian Random Field based cluster inference with a height threshold of $Z > 2.3$ and a cluster significance threshold of $P < 0.05$. To control for the possible effect of interindividual differences in gray matter density on BOLD (17), individual gray matter density maps were included in the FEAT GLM as a confound regressor. Gray matter maps were extracted using FMRIB's Automated Segmentation Tool (FAST), registered in standard space, and smoothed to match the fMRI data (18).

Generation of White Matter Tracts Using Tractography. Individual tractography was performed in a separate group of 10 young normal controls (6 males, mean age = 23 ± 2.5). Tracts were generated between 10-mm-radius spherical regions of interest placed based on the peak activation or deactivation during correct stop trials vs. go trials (Table S4) using probalistic tractography in FSL. To avoid the potential problems associated with probabilistic tractography in patients with abnormal white matter, we followed a similar approach to that described by Hua et al. (19). FA maps were nonlinearly warped and registered to the 1-mm *FMRIB* MNI FA template, by using FSL FNIRT, and the obtained transformations were used to bring the individual tractography outputs to the standard space. The projected tracts were then averaged across the 10 subjects. For the resulting maps, a conservative threshold corresponding to 5% of voxels with highest connectivity values was used. For each tract connecting a pair of regions A and B, tractography was performed from A to B and from B to A. The two resulting thresholded tracts were then averaged and binarized.

The seven tracts obtained with this procedure were used as masks for the ROI analysis of white matter integrity in TBI patients and in a group of 30 age-matched controls distinct from the one used to generate the tracts. Tracts were projected into each individual's DTI space by using the inverse of the nonlinear transformation used to align the subject-space FA maps to the MNI template. To reduce the possibility of sampling nonwhite matter regions the transformed tracts were constrained within a white matter tracts mask derived from TBSS (ref. 20; Fig. 2*C*). A mean FA image was created by using the FA maps aligned to the MNI template and then thinned to generate a "skeleton" representing the center of the tracts. The aim was to include only the core of the tract, while excluding peripheral parts of the fiber tract that show pronounced interindividual variability. The resulting FA skeleton outlines the center of large white matter tracts and so allows the calculation of white matter integrity to avoid sampling the edges of these tracts, which are more prone to artifacts, such as partial volume effects due the edge of the ventricles. The obtained maps were binarized and applied to the FA maps to obtain one mean FA value per tract and per subject. Mean FA values were thus calculated from the area of overlap between the whole white matter skeleton and the mask of the particular tract in individual space. We then used linear regression to derive FA values corrected for any effects of age in the analyses reported. Back-projections of the white matter skeleton and the rAI–preSMA/dACC ROI onto each patient's and control's individual FA maps can be viewed in Figs. S3 and S4. This shows that the back-projection of the skeleton and the rAI–preSMA/dACC tract are well constrained to the white matter in each subject's individual DTI space.

1. Boehler CN, Appelbaum LG, Krebs RM, Hopf JM, Woldorff MG (2010) Pinning down response inhibition in the brain—conjunction analyses of the stop-signal task. *Neuroimage* 52:1621–1632.
2. Delis DC, Kaplan E, Kramer JH (2001) *Delis-Kaplan executive function system (D-KEFS): Examiner's manual* (The Psychological Corporation, San Antonio, TX).
3. Malec JF, et al. (2007) The mayo classification system for traumatic brain injury severity. *J Neurotrauma* 24:1417–1424.
4. Scheid R, Preul C, Gruber O, Wiggins C, von Cramon DY (2003) Diffuse axonal injury associated with chronic traumatic brain injury: evidence from T2*-weighted gradient-echo imaging at 3 T. *AJNR Am J Neuroradiol* 24:1049–1056.
5. Gentry LR, Godersky JC, Thompson B (1988) MR imaging of head trauma: review of the distribution and radiopathologic features of traumatic lesions. *AJR Am J Roentgenol* 150:663–672.
6. Wechsler D (1999) *WASI: Wechsler Abbreviated Scale of Intelligence* (The Psychological Corporation, San Antonio, TX).
7. Delis DC, Kaplan E, Kramer JH (2001) *Delis-Kaplan Executive Function System* (Psychological Corporation, San Antonio, TX).
8. Reitan R (1958) The validity of the Trail Making test as an indicator of organic brain damage. *Percept Mot Skills* 8:271–276.
9. Wechsler D (1997) *Wechsler Memory Scale- Third Edition: Administration and Scoring Manual* (Psychological Corporation, San Antonio, TX).
10. Baddeley AD, Emslie H, Nimmo-Smith I (1994) *Doors and People Test: A Test of Visual and Verbal Recall and Recognition* (Thames Valley Test Company, Bury-St-Edmunds, United Kingdom).
11. Logan GD, Cowan WB, Davis KA (1984) On the ability to inhibit simple and choice reaction time responses: a model and a method. *J Exp Psychol Hum Percept Perform* 10:276–291.
12. Alderson RM, Rapport MD, Sarver DE, Kofler MJ (2008) ADHD and behavioral inhibition: A re-examination of the stop-signal task. *J Abnorm Child Psychol* 36: 989–998.
13. Leotti LA, Wager TD (2010) Motivational influences on response inhibition measures. *J Exp Psychol Hum Percept Perform* 36:430–447.
14. Smith SM (2002) Fast robust automated brain extraction. *Hum Brain Mapp* 17: 143–155.
15. Smith SM, et al. (2004) Advances in functional and structural MR image analysis and implementation as FSL. *Neuroimage* 23(Suppl 1):S208–S219.
16. Beckmann CF, Jenkinson M, Smith SM (2003) General multilevel linear modeling for group analysis in FMRI. *Neuroimage* 20:1052–1063.
17. Oakes TR, et al. (2007) Integrating VBM into the General Linear Model with voxelwise anatomical covariates. *Neuroimage* 34:500–508.
18. Filippini N, et al. (2009) Distinct patterns of brain activity in young carriers of the APOE-epsilon4 allele. *Proc Natl Acad Sci USA* 106:7209–7214.
19. Hua K, et al. (2008) Tract probability maps in stereotaxic spaces: Analyses of white matter anatomy and tract-specific quantification. *Neuroimage* 39:336–347.
20. Smith SM, et al. (2006) Tract-based spatial statistics: Voxelwise analysis of multi-subject diffusion data. *Neuroimage* 31:1487–1505.

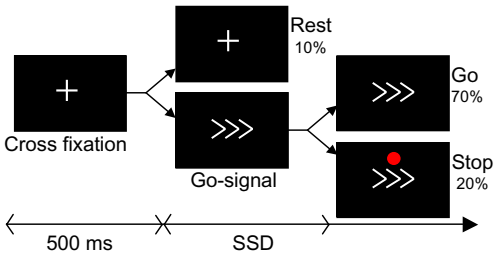

Fig. S1. Stop signal task. Trials start with a fixation cross presented for 500 ms followed by a go-stimulus (a right or left pointing arrow). On 10% of the trials, the cross fixation remained on the screen (Rest trials); 30% of the trials involve an unpredictable stop-signal (red dot) presented at a variable delay following the go-signal (the stop signal delay; SSD).

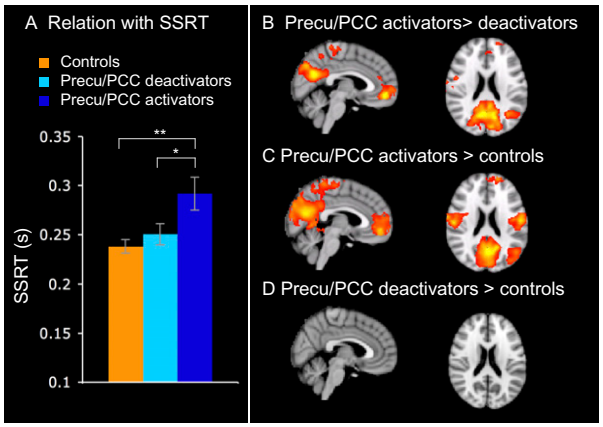

Fig. S2. The behavioral relevance of DMN abnormality following TBI. Patients were split into "activators" and "deactivators" based on the presence of deactivation within the precu/PCC. (*A*) SSRT differences between the two groups of patients and controls. $*P < 0.05$; $**P < 0.005$. (*B–D*) Whole-brain comparison of BOLD signal change for the contrast StC > Go between patients with no precu/PCC deactivation ($n = 20$; activators) and patients with precu/PCC deactivation ($n = 26$; deactivators) (*B*); activators and controls (*C*); and deactivators and controls (*D*). $Z = 2.3$; $P < 0.05$.

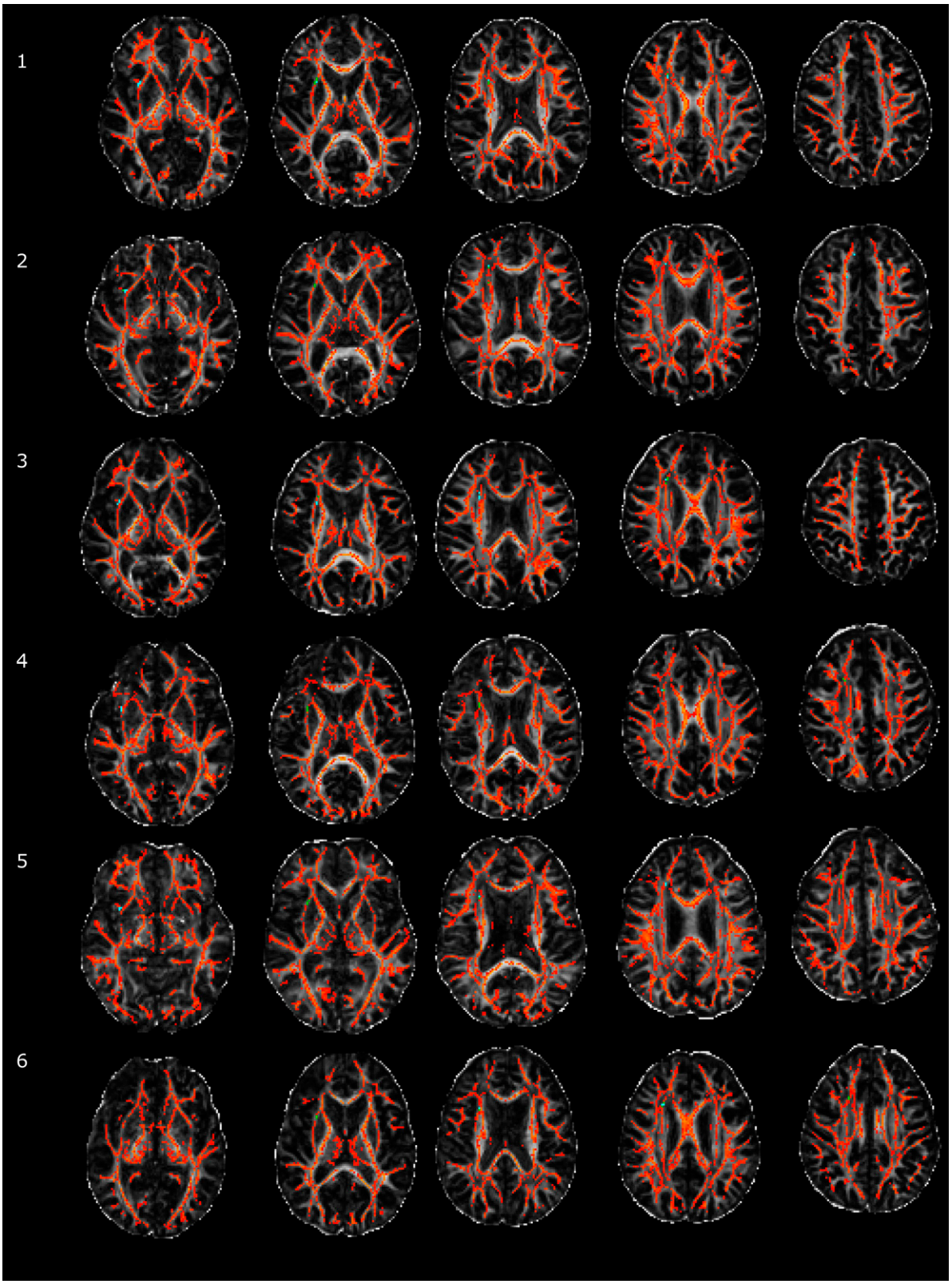

Fig. S3. (Continued)

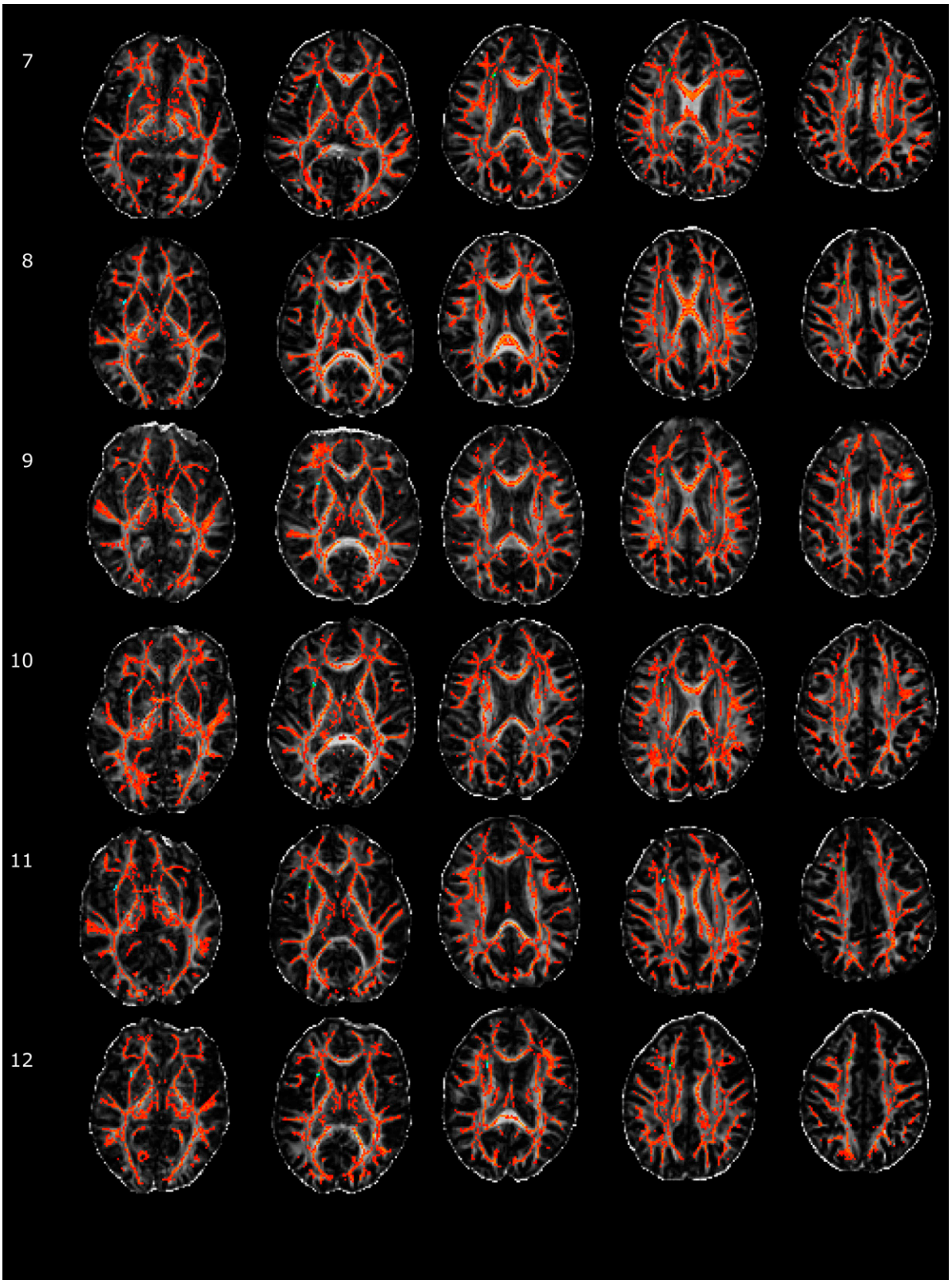

Fig. S3. (Continued)

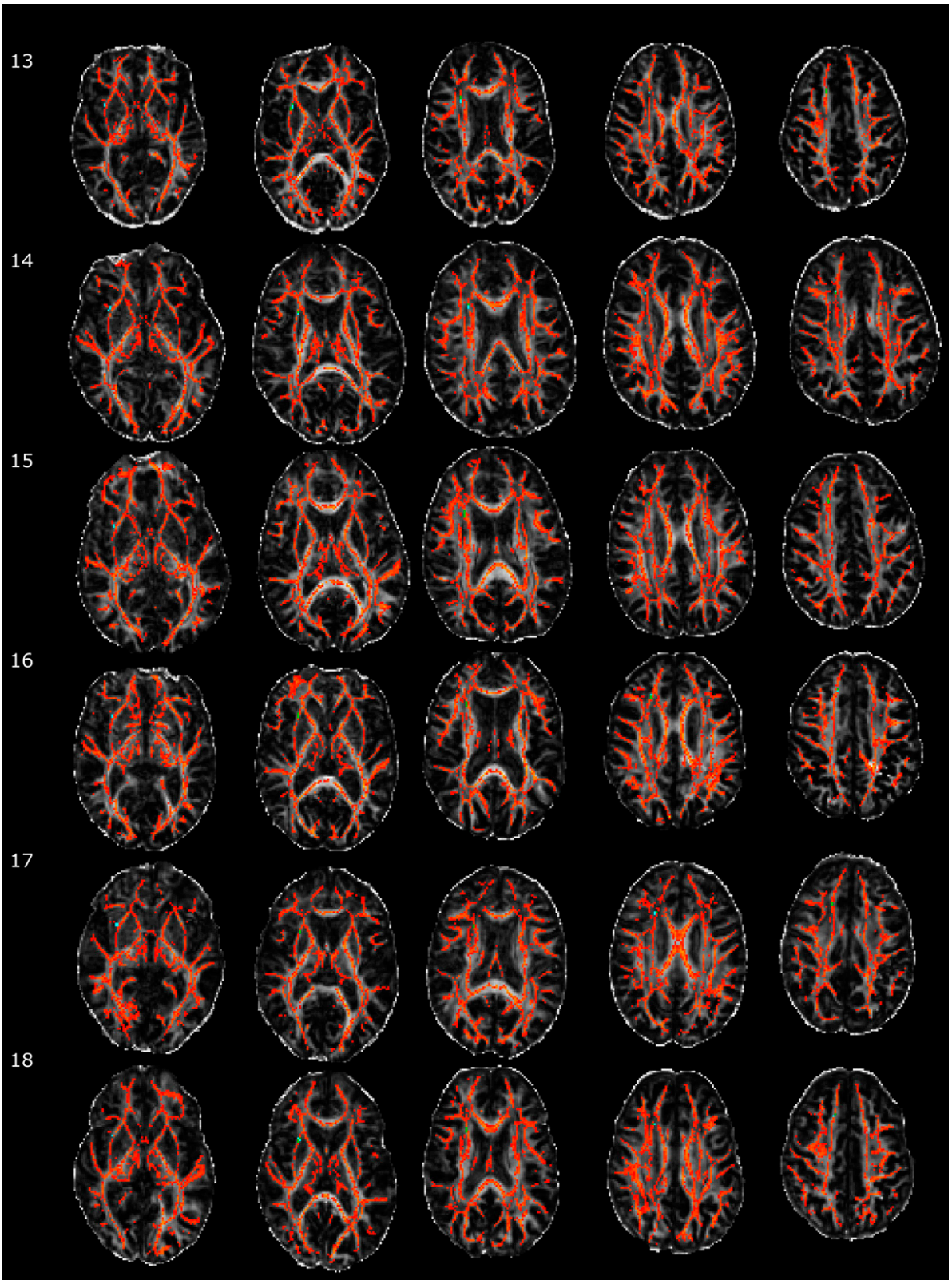

Fig. S3. (Continued)

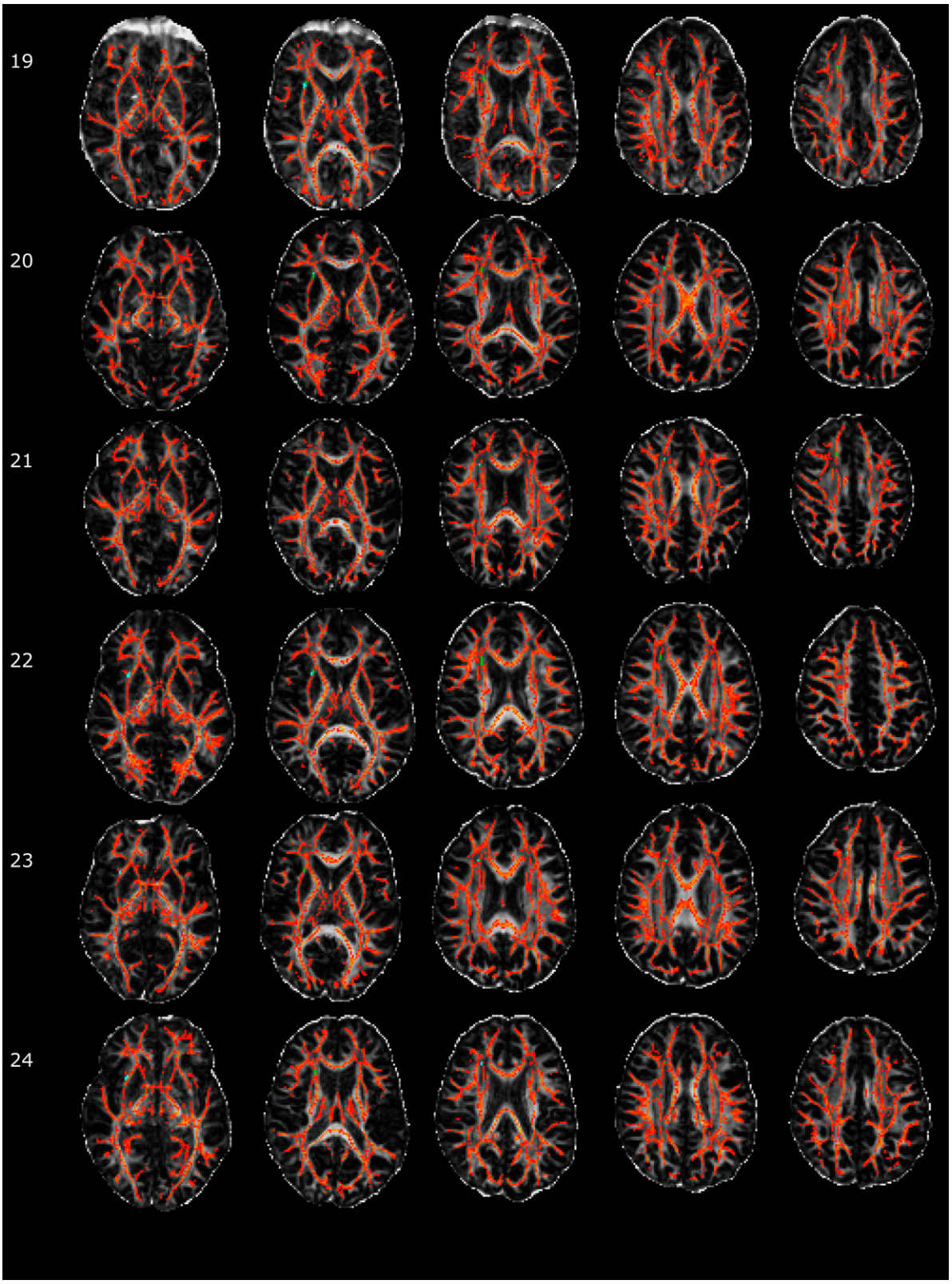

Fig. S3. (Continued)

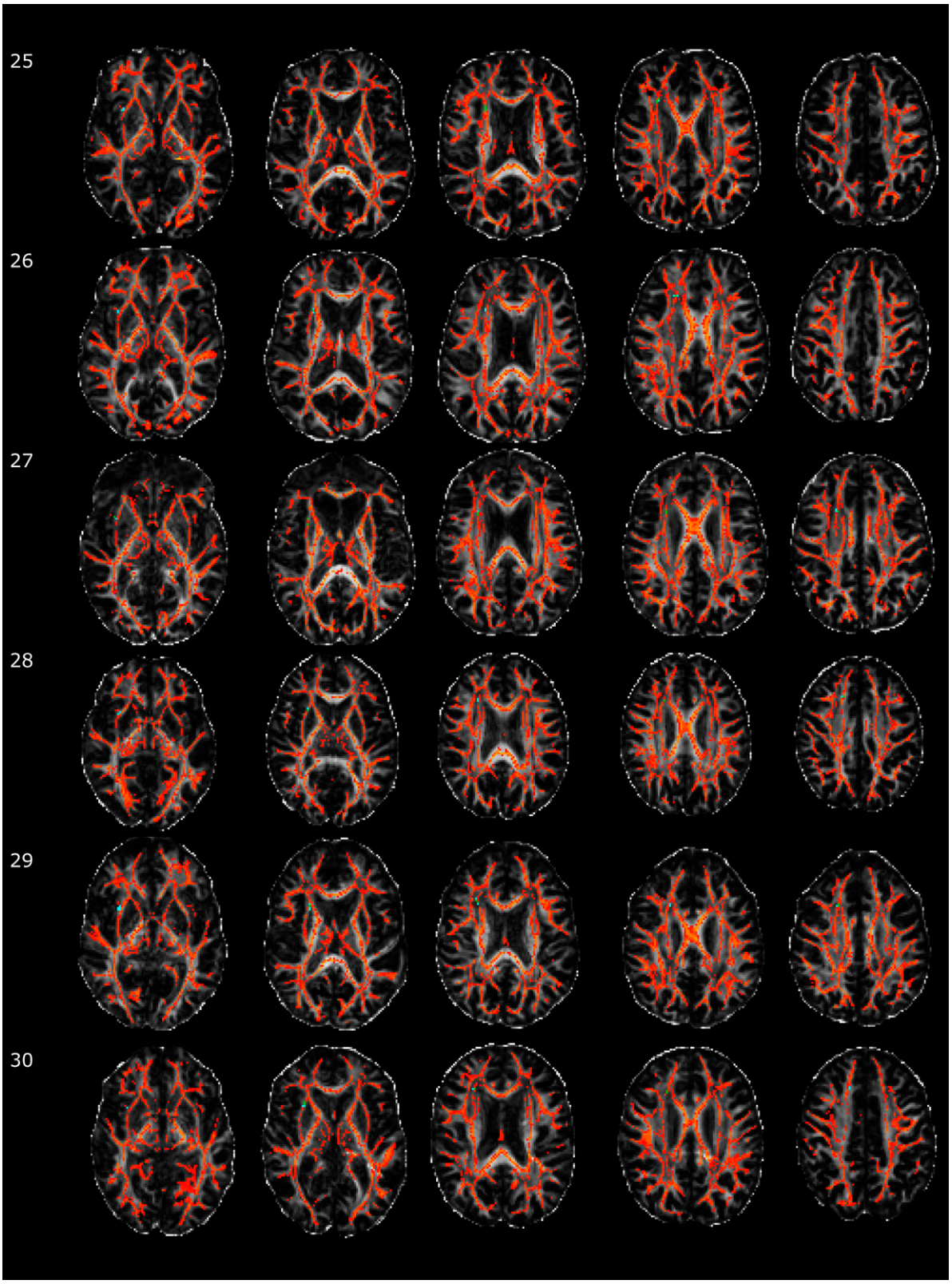

Fig. S3. (Continued)

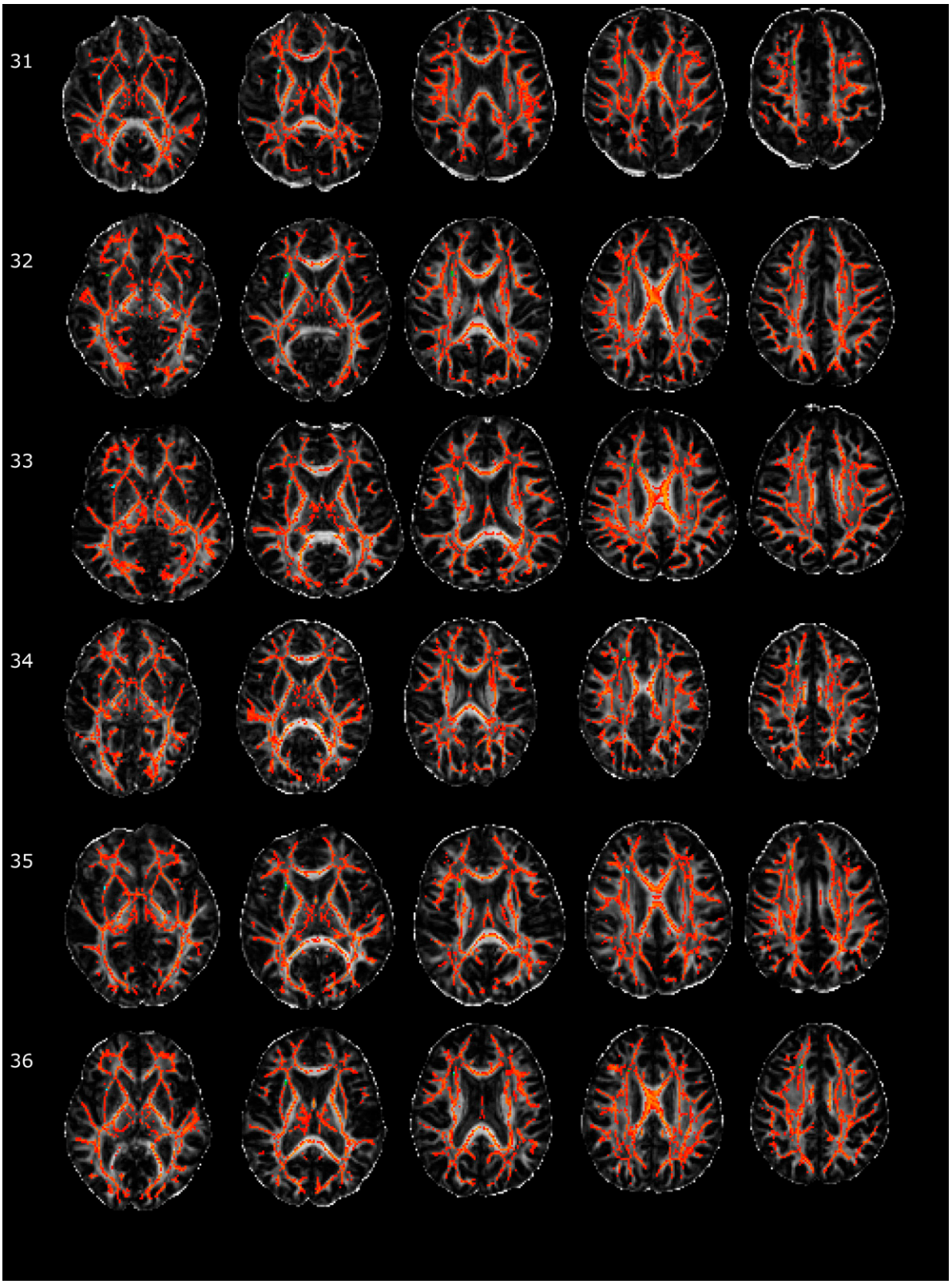

Fig. S3. (Continued)

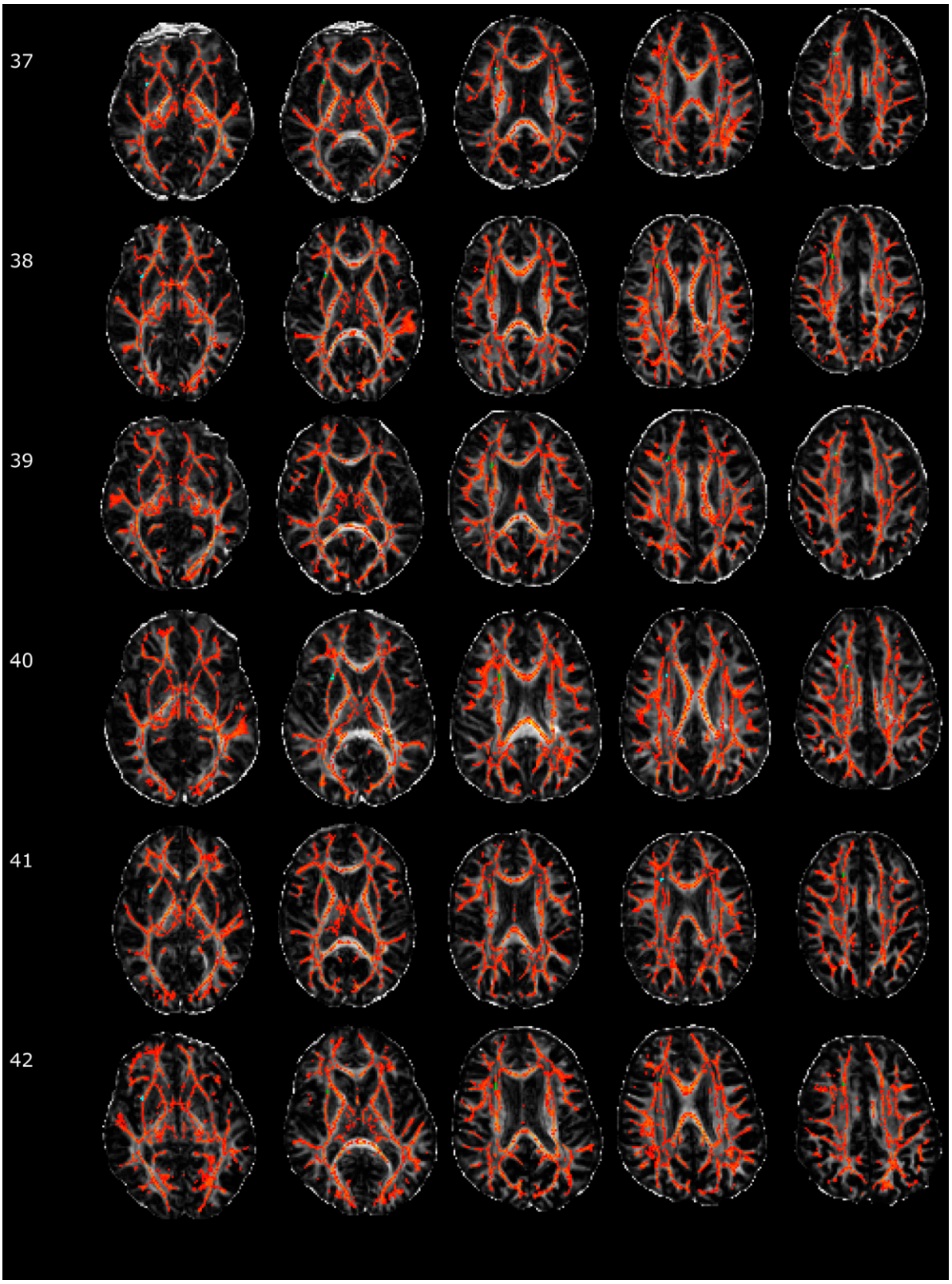

Fig. S3. (Continued)

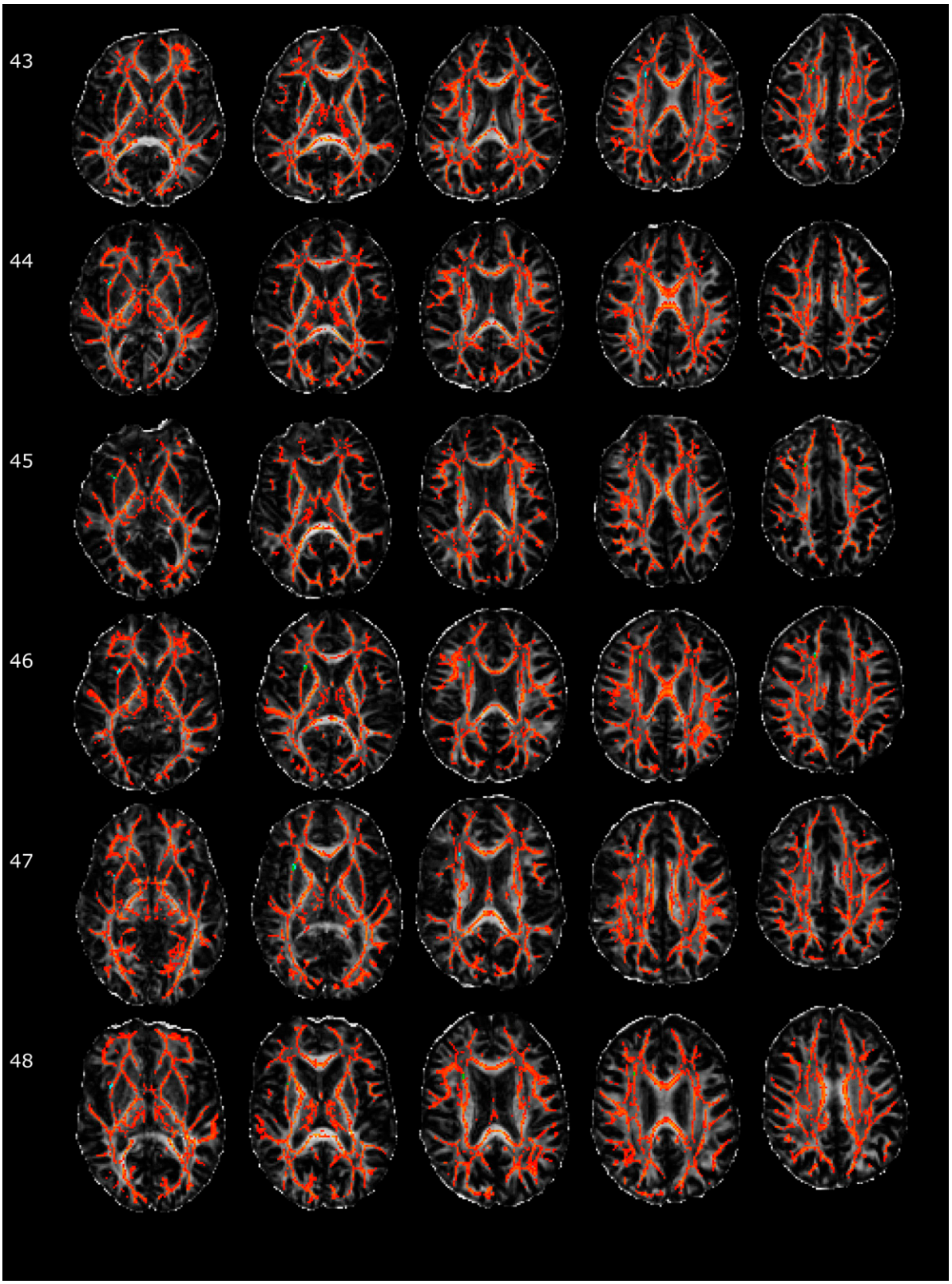

Fig. S3. (Continued)

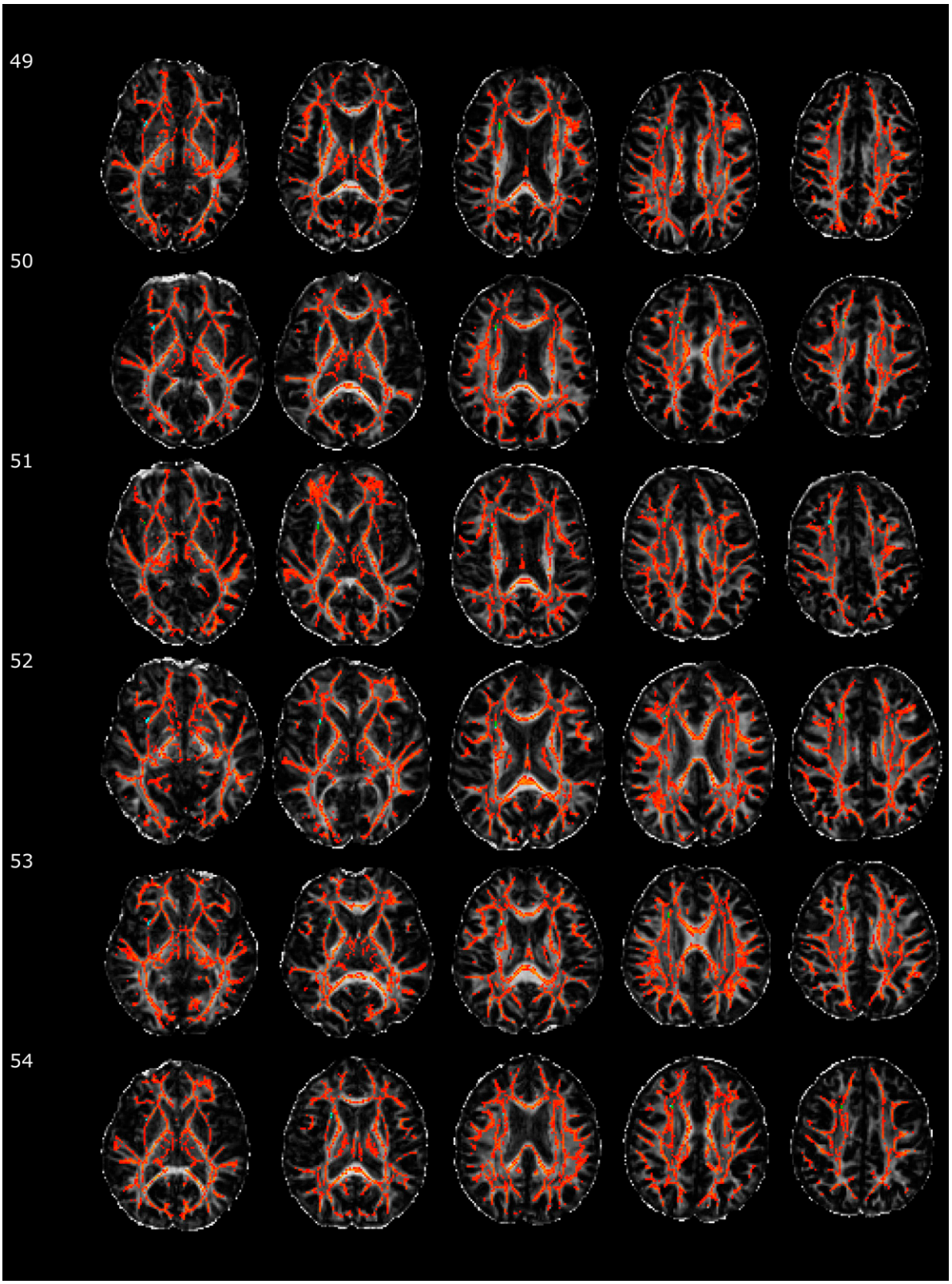

Fig. S3. Axial views of the TBSS white matter skeleton (orange-red) and the rAI–preSMA/dACC tract (blue) projected onto each patient's raw FA map using nonlinear warping.

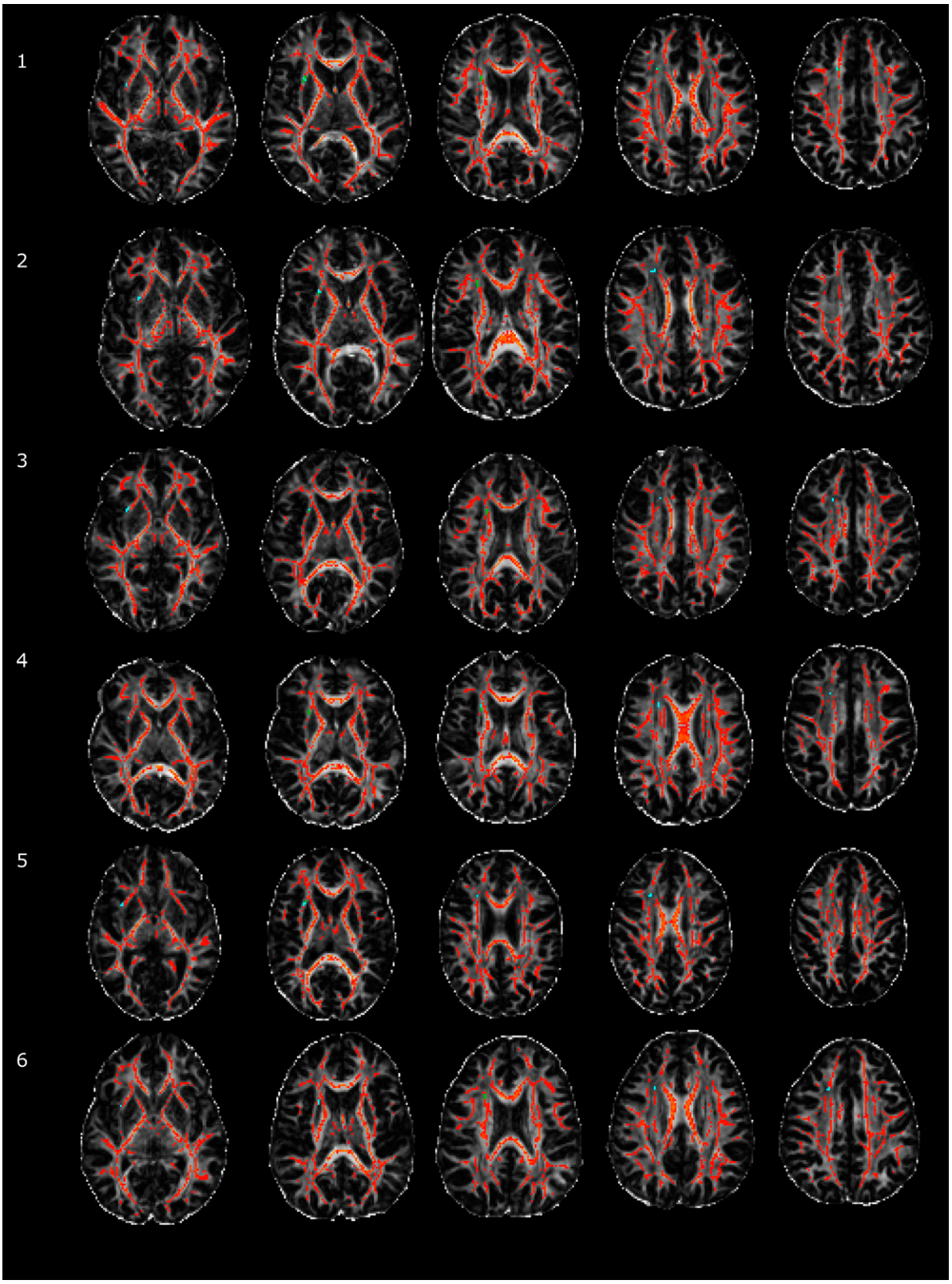

Fig. S4. (Continued)

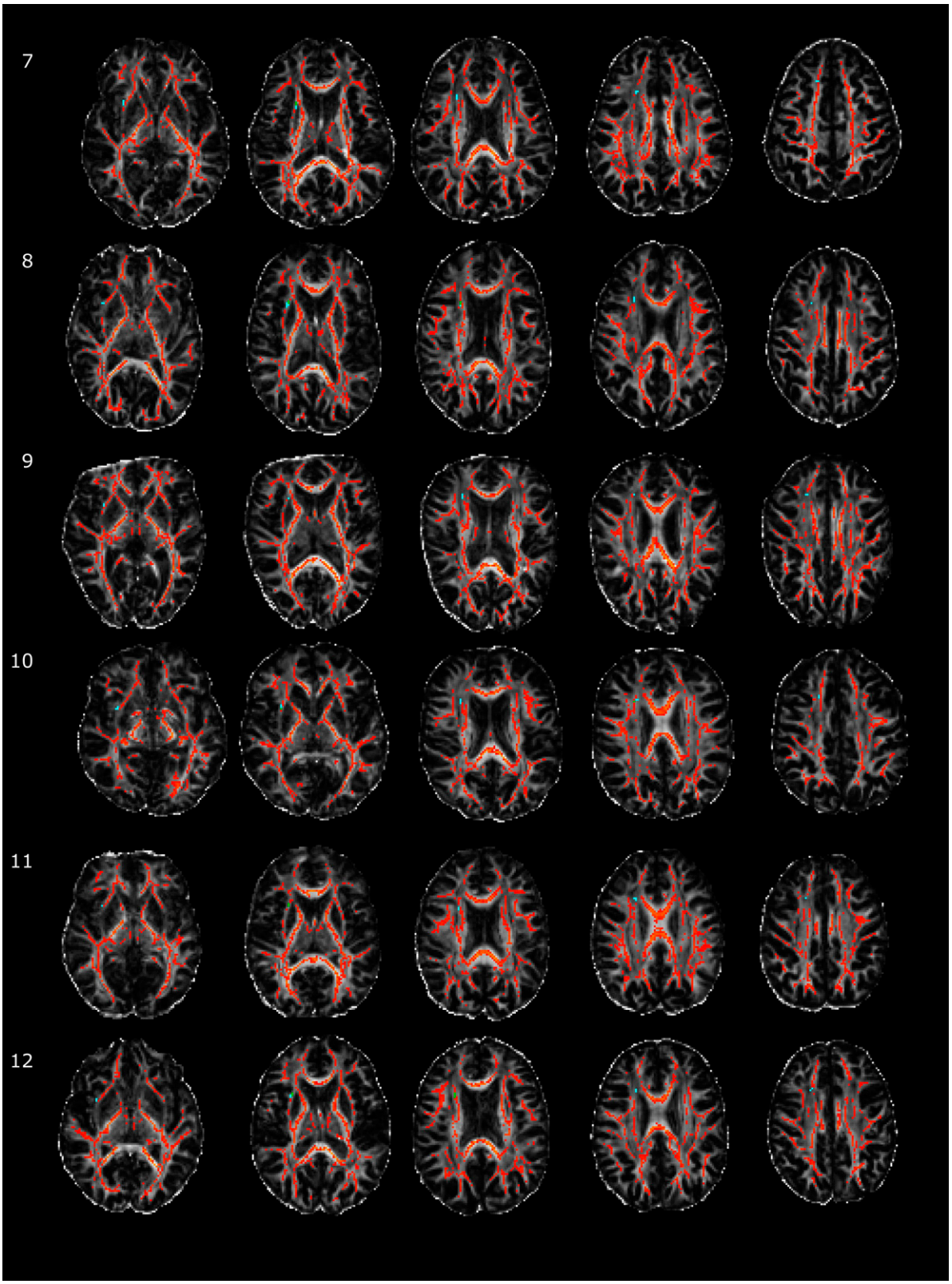

Fig. S4. (Continued)

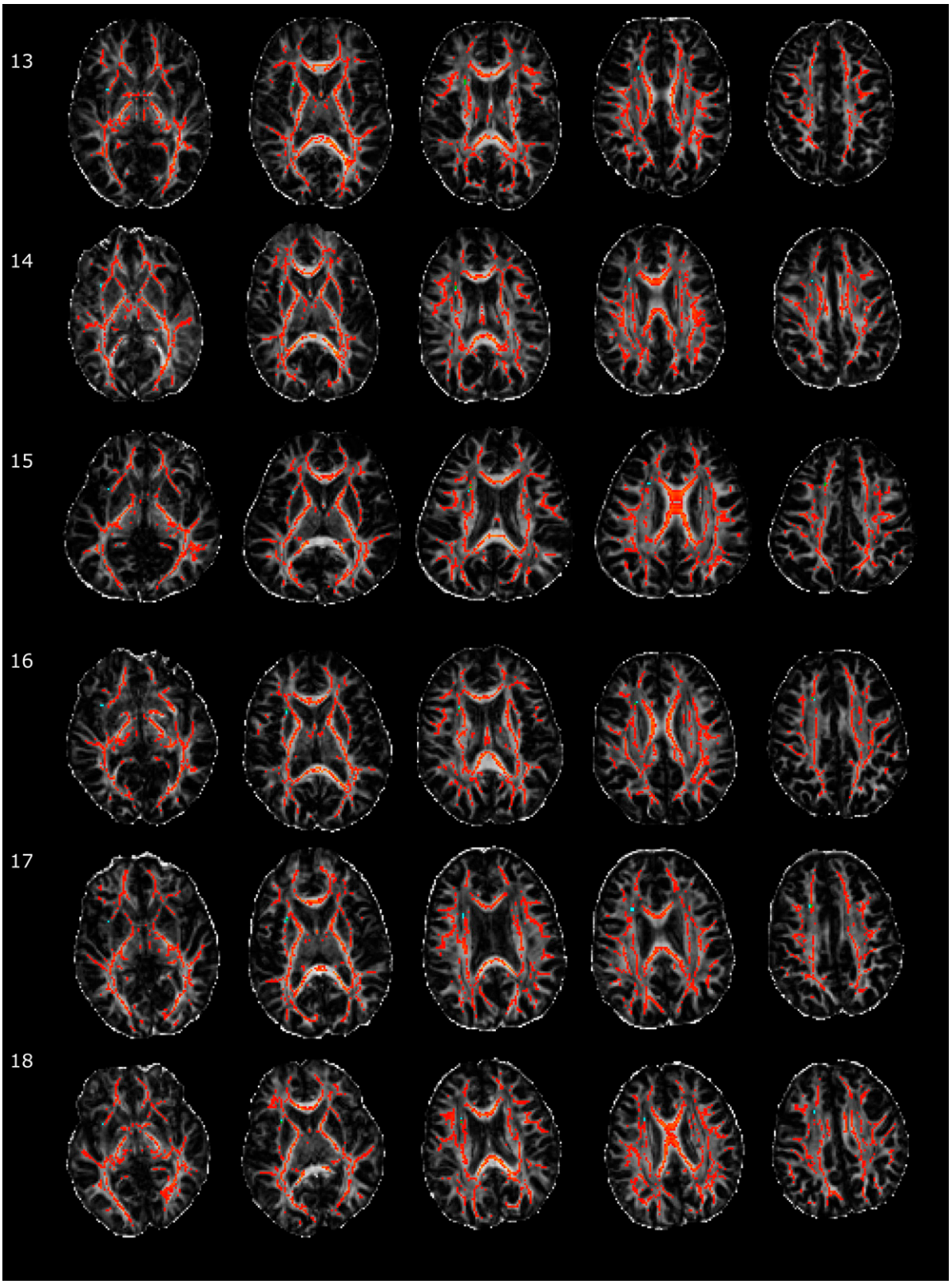

Fig. S4. (Continued)

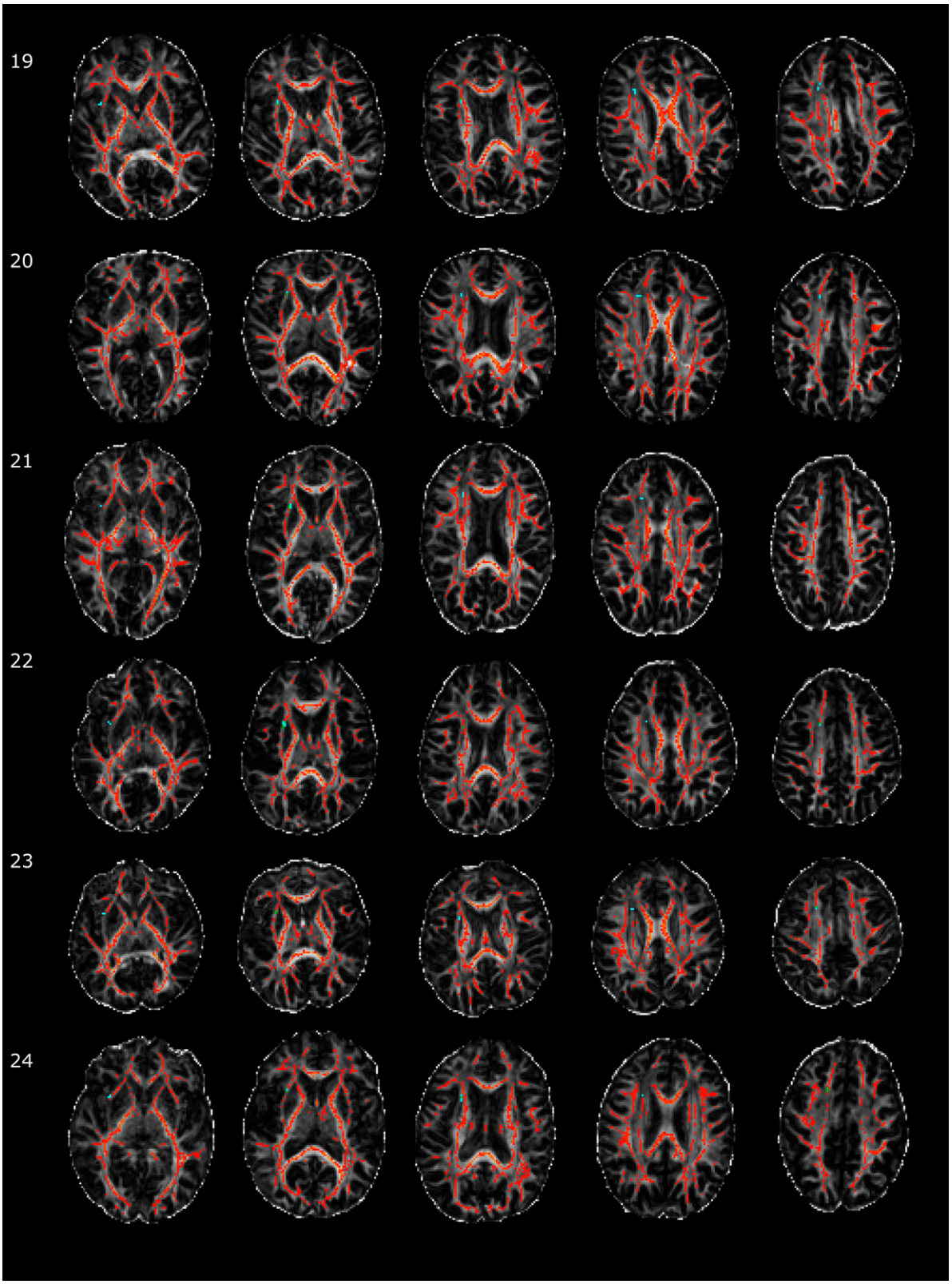

Fig. S4. (Continued)

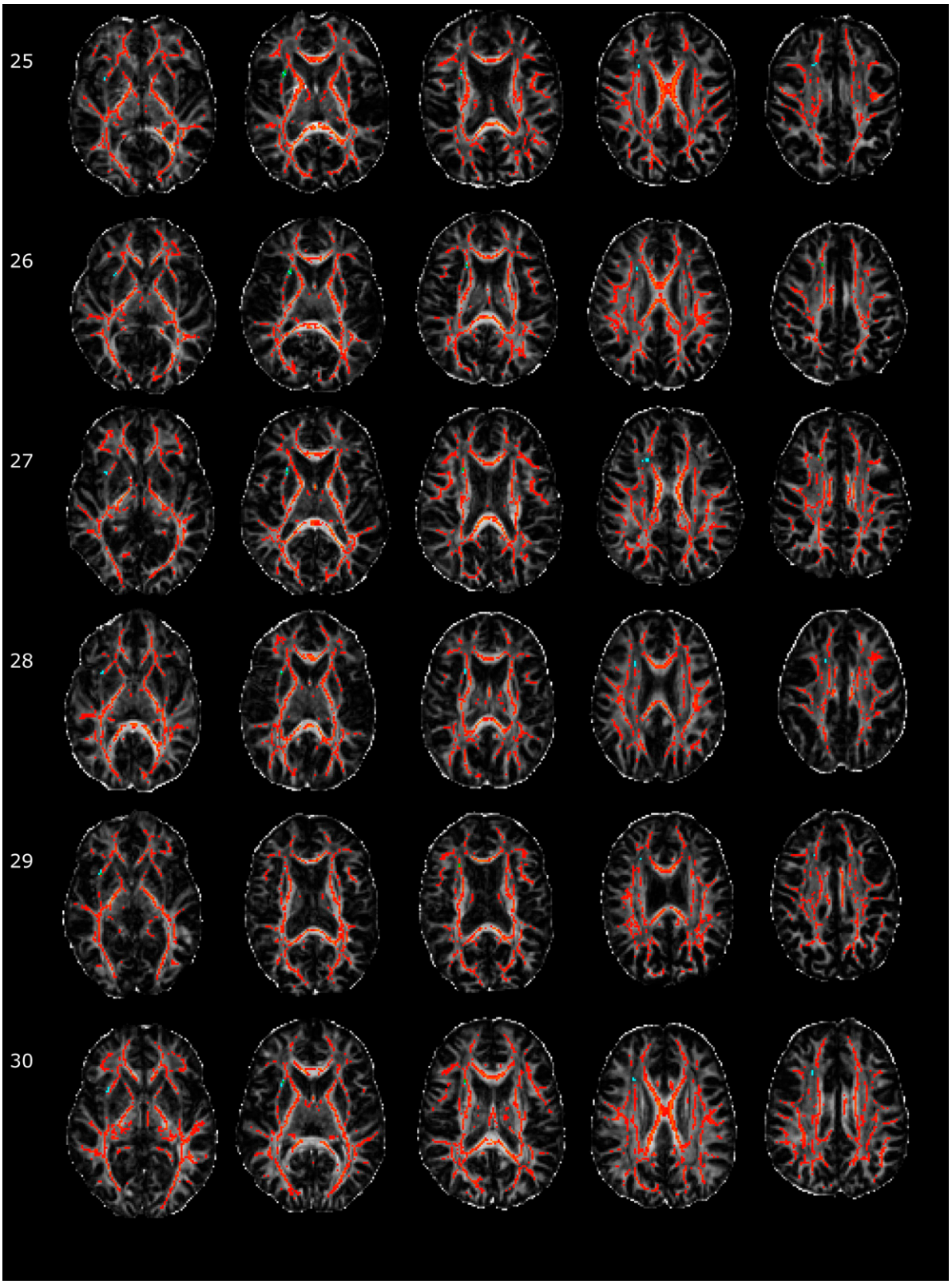

Fig. S4. Axial views of the TBSS white matter skeleton (orange-red) and the rAI–preSMA/dACC tract (blue) projected onto each control's raw FA map using nonlinear warping.

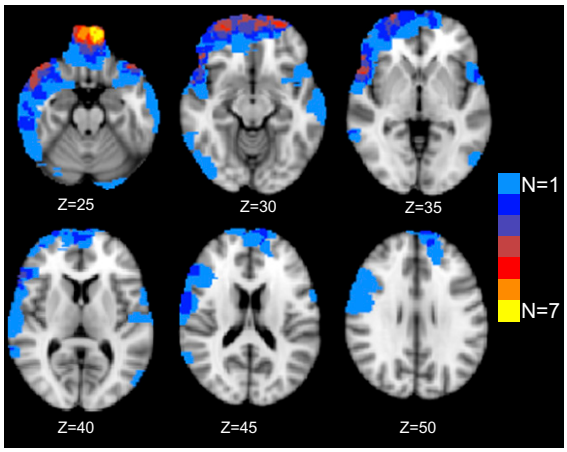

Fig. S5. Overlap map of lesions visible on T1 MR imaging. The color of the map represents the number of patients with a lesion in that area.

Table S1. Neuropsychological results for patients and controls

Cognitive variable	Controls, mean ± SD	Patients, mean ± SD
Similarities raw score	35.1 ± 6.2	38.7 ± 3.8▪▪▪
Matrix reasoning raw score	26.5 ± 4.2	27.4 ± 4.8
Verbal fluency letter fluency	48.5 ± 12.0	44.1 ± 11.2
Stroop color naming, s	32.2 ± 14.1	34.0 ± 8.9
Stroop word reading, s	29.6 ± 5.1	23.4 ± 4.8
Stroop Inhibition, s	22.4 ± 4.2	58.3 ± 20.9**
Stroop inhibition-switching, s	51.5 ± 18.7	68.4 ± 21.2**
Trail making test A, s	21.5 ± 5.7	27.4 ± 10.4*
Trail making test B, s	53.7 ± 38.5	64.7 ± 35.1
Digit span forward	11.2 ± 2.0	10.6 ± 2.2
Digit span backward	7.6 ± 1.7	7.4 ± 2.3
Logical memory I first recall total	28.1 ± 8.4	27.9 ± 6.5
Logical memory I recall total	45.1 ± 12.8	45.5 ± 8.7
Logical memory II recall total	26.6 ± 8.5	29.4 ± 7.0
People test immediate total	27.5 ± 6.2	24.1 ± 5.6
People test delayed total	9.2 ± 3.6	8.8 ± 2.3

Neuropsychological results for TBI patients compared with an age-matched control group. The Color Naming, Word Reading, Inhibition/Switching, and Letter Fluency tests are from the Delis-Kaplan Executive Function System. Significant differences between patients and controls shown by *$P < 0.05$ and **$P < 0.005$. Stroop test refers to the D-KEFS Color-Word Interference Test.

Table S2. Behavioral results for TBI patients and controls on the two SST runs

	First run SST	Second run SST	Mean 2 runs
Patients			
Mean RT, ms	484 ± 120	481 ± 171	483 ± 116
Go accuracy, %	95.7 ± 5.0*	95.3 ± 5.6*	95.5 ± 4.8*
Stop accuracy, %	49.8 ± 3.3	49.4 ± 3.3	49.6 ± 2.6
Neg. feedback	8.8 ± 5.9	9.0 ± 5.2	8.9 ± 5.1
IIV	190 ± 60	187 ± 54	188 ± 54
SSRT, ms	265 ± 64*	272 ± 73*	268 ± 67*
Controls			
Mean RT, ms	443 ± 50	443 ± 110	443 ± 106
Go accuracy, %	98.2 ± 1.6	98.6 ± 1.5	98.4 ± 1.5
Stop accuracy, %	48.5 ± 3.8	50.6 ± 3.3	49.5 ± 2.2
Neg. feedback	10.9 ± 5.9	11.1 ± 4.3	11.2 ± 4.3
IIV	186 ± 35	176 ± 48	181 ± 37
SSRT, ms	234 ± 34	239 ± 38	238 ± 32

Behavioral results for the SST. Only behavioral results from subjects whose SSRT could be estimated on both SST runs are presented (22 controls and 45 patients). Mean reaction times (RT) for correct Go trials, percentage accuracy on go and stop trials, number of negative feedbacks, intraindividual variability of go reaction time (IIV), and SSRT are reported (± SD). *$P < 0.05$ (significant differences between patients and controls).

Table S3. Local maxima of brain activations differences between control and patients for the contrast Go vs. StC

	MNI coordinates			
Controls > Patients, Go > StC	*x*	*y*	*Z*	Z score
L parietal operculum cortex	−50	−28	18	4.88
R central opercular cortex	66	−6	6	4.48
L central opercular cortex	−62	−12	8	4.04
R posterior Insula	38	−16	6	4.08
L posterior Insula	−34	−14	0	3.96
Precuneus	−2	−66	18	4.48
L medial prefrontal cortex	−12	56	12	3.68
L hippocampus	−20	−12	−18	3.99
L amygdala	−22	−8	−16	4.03

Local maxima are presented for the comparison of brain regions showing increased activation on go trials, or decreased activation on correct stop trials between controls and patients, with associated *Z*-values. MNI, Montreal Neurological Institute; R, right; L, left.

Table S4. MNI coordinates for seed and termination tractography masks

	x	*y*	*z*
preSMA	20	6	62
rIFG	44	18	16
rTPJ	58	−40	26
rFEF	32	8	48
rIPS	30	−62	48
dACC	0	22	46
rAI	36	24	−6
lAI	−36	18	0
lmPFC	−8	54	22
lprecu	−4	−60	20
rmPFC	8	54	22
rprecu	4	−60	20

MNI coordinates of seeds/termination regions used for tractography, based on peak activation/deactivation for the contrast StC > Go in controls.